ELSEVIER

Journal of Fluids and Structures 23 (2007) 1047–1063

JOURNAL OF FLUIDS AND STRUCTURES

www.elsevier.com/locate/jfs

Symmetric vortex shedding in the near wake of a circular cylinder due to streamwise perturbations ☆

E. Konstantinidis[a,*], S. Balabani[b]

[a]*Department of Engineering and Management of Energy Resources, University of Western Macedonia, Bakola and Sialvera, Kozani 50100, Greece*

[b]*Department of Mechanical Engineering, King's College London, Strand, London WC2R 2LS, UK*

Received 24 February 2006; accepted 10 March 2007
Available online 16 May 2007

Abstract

Symmetric perturbations imposed on cylinder wakes may result in a modification of the vortex shedding mode from its natural antisymmetric, or alternating, to a symmetric one where twin vortices are simultaneously shed from both sides of the cylinder. In this paper, the symmetric mode in the wake of a circular cylinder is induced by periodic perturbations imposed on the in-flow velocity. The wake field is examined by PIV and LDV for Reynolds numbers about 1200 and for a range of perturbation frequencies between three and four times the natural shedding frequency of the unperturbed wake. In this range, a strong competition between symmetric and antisymmetric vortex shedding occurs for the perturbation amplitudes employed. The results show that symmetric formation of twin vortices occurs close to the cylinder synchronized with the oscillatory component of the flow. The symmetric mode rapidly breaks down and gives rise to an antisymmetric arrangement of vortex structures further downstream. The downstream wake may or may not be phase-locked to the imposed oscillation. The number of cycles for which the symmetric vortices persist in the near wake is a probabilistic function of the perturbation frequency and amplitude. Finally, it is shown that symmetric shedding is associated with positive energy transfer from the fluid to the cylinder due to the fluctuating drag.

1. Introduction

The investigation of bluff-body/near-wake interactions is of great importance not only as a fundamental problem in fluid mechanics but also for flow and/or vibration control in engineering applications. The wake of a circular cylinder has been the focal point of research over many decades and various types of fluid–structure interaction have been considered in numerous studies, e.g., rectilinear oscillations of the cylinder, rotational or orbital oscillations, flow or sound forcing, surface suction or blowing, in which an externally forced periodic perturbation interacts with the intrinsic instability of the wake, i.e., vortex shedding. There are many common features resulting from such interactions as a function of the perturbation frequency and amplitude, the most important being the synchronization of the wake frequency to that of the imposed perturbation often termed *vortex shedding lock-on* (Griffin and Hall, 1991).

☆An earlier version of this paper was presented in the seventh FSI, AE & FIV + N Symposium, held within the 2006 ASME PVP Conference in Vancouver, BC, Canada.

*Corresponding author. Tel.: +30 24610 56754.
E-mail address: ekonstantinidis@uowm.gr (E. Konstantinidis).

0889-9746/$ - see front matter © 2007 Elsevier Ltd. All rights reserved.
doi:10.1016/j.jfluidstructs.2007.03.002

Nevertheless, a broad distinction can be made between perturbations which are symmetric or antisymmetric with respect to a plane aligned in the flow direction and passing through the cylinder axis. A unique phenomenon relating to the former type of perturbations is the induction of symmetric shedding of 'twin' vortices in the near wake when, for example, a cylinder oscillates in the streamwise direction or, equivalently, when the flow velocity around a fixed cylinder has an oscillatory component superimposed on the mean. This mode of vortex shedding is only possible when the imposed perturbation has a symmetric component, since the intrinsic instability of the wake associated with alternating vortex shedding is purely antisymmetric, i.e., it exhibits a spatio-temporal symmetry.

Symmetric vortex shedding has been observed in many investigations and a summary of related observations either from experimental studies with the aid of flow visualization or from numerical simulations is provided in Table 1. The list might not be complete but the aim here is to review briefly the current state of understanding. The early experiments of Griffin and Ramberg (1976) did not reveal a symmetric mode of vortex shedding and their study is not included in Table 1. The cylinder was oscillated at frequencies near twice the intrinsic shedding frequency of the unforced wake (f_o), for which it is now recognized that vortex shedding occurs in a purely antisymmetric mode (Griffin and Hall, 1991; Konstantinidis et al., 2005b). Ongoren and Rockwell (1988) conducted a systematic study of the flow structure in the near wake of a cylinder oscillating at various angles to the flow direction. With the exemption of oscillations in the cross-stream direction for which the imposed perturbation does not have a symmetric component, they have observed a competition and switching between symmetric and antisymmetric modes of vortex formation in the near wake based on the examination of a large number of visualization images. The number of occurrences of each mode is a function of the excitation (oscillation) frequency, f_e, and angle of cylinder oscillation relative to the flow. For streamwise oscillations, the symmetric shedding mode is amplified for $f_e/f_o = 1$ and prevails in the range $f_e/f_o = 3$–4. Yokoi and Kamemoto (1994) also observed the symmetric vortex formation for $f_e/f_o \simeq 1$ and relatively large amplitudes of oscillation, but they additionally noted that the symmetric shedding of vortices may lead to an antisymmetric as well as a symmetric downstream wake. In contrast, the experiments of Gau et al. (2001) at relatively small amplitudes of oscillation, revealed symmetric shedding only for $f_e/f_o = 3$ but not for $f_e/f_o = 1$. More recently, Nishihara et al. (2005) measured the fluid forces acting on a cylinder and visualized the wake patterns behind it when it was forced to oscillate in the streamwise direction. The observed wake patterns were similar to those of Ongoren and Rockwell (1988) as a function of the frequency ratio, despite the differences in amplitude and Reynolds number. Related numerical work has also provided evidence of the symmetric mode for $f_e/f_o \simeq 2.6$ (Rao et al., 1992) and $f_e/f_o = 3$ (Lecointe and Piquet, 1989; Liu and Fu, 2003), though the correspondence of the wake flow predicted from such two-dimensional simulations to the

Table 1
Summary of observations of symmetric vortex shedding from flow visualization and numerical simulation

Researchers	Method	Perturbation	Medium	Re	f_e/f_o	A*
King et al. (1973)	Dye	Self-excited oscillation[a]	Water	$5–15 \times 10^3$	2–4.2	0–0.2
Barbi et al. (1986)	Smoke	Flow forcing	Air	40 000	0.7	0.2
Barbi et al. (1986)	Dye	Flow forcing	Water	3000	1	0.036
Detemple-Laake and Eckelman (1989)	Smoke	Sound waves	Air	152	1.4–1.7	na
Ongoren and Rockwell (1988)	Hydrogen bubble	Forced cylinder oscillation	Water	855	0.5–4	0.13
Lecointe and Piquet (1989)	Numerical	Forced cylinder oscillation	—	855	3	0.13
Al-Asmi and Castro (1992)	Smoke[b]	Flow forcing	Air	1640	4	0.15
Rao et al. (1992)	Numerical	Forced cylinder oscillation	—	1000, 4000	2.5	0.2
Yokoi and Kamemoto (1994)	Smoke	Forced cylinder oscillation	Water	490	0.9	0.1
Zhou and Graham (2000)	Numerical	Oscillatory plus mean flow	—	400–600	1.5–2.5	0.32–0.48
Gau et al. (2001)	Smoke	Forced cylinder oscillation	Air	1600	2.5–3	0.05
Okajima et al. (2000)	Smoke	Self-excited oscillation	Air	9000	2.4	0.08
Liu and Fu (2003)	Numerical	Forced cylinder oscillation	—	200	2.5	0.50
Liu and Fu (2003)	Numerical	Forced cylinder oscillation	—	855	2.9	0.26
Jauvtis and Williamson (2004)	PIV	2-d.o.f. self-excited oscillation	Water	1600	2.4	0.10
Nishihara et al. (2005)	LIF	Forced cylinder oscillation	Water	17 000	3.2–4.4	0.05
Xu et al. (2006)	LIF	Forced cylinder oscillation	Water	500	1.7–3.1	0.50

PIV = particle image velocimetry.
LIF = laser-induced fluorescence.
na = not available.
[a]Cantilevered cylinder.
[b]Flat plate.

experimental observations may be questioned. Finally, a symmetric 'binary' vortex street which consists of two pairs of vortices per cycle was recently discovered by Xu et al. (2006) over a range of excitation frequencies $f_e/f_o = 1.7$–3.1 and very high amplitudes. In their experiments, however, the streamwise oscillation of the cylinder is so high that the relative velocity between the cylinder and the flow is changing sign over part of the cycle, a fact that has till now remained unnoticed. It should also be noted that for correspondingly high oscillation amplitudes, Cetiner and Rockwell (2001) have not reported symmetric vortex formation.

Pertinent to the present study is the case where the cylinder is fixed and the in-flow has an oscillatory component superimposed on the mean. This type of perturbation is equivalent to the streamwise oscillation of the cylinder in a time-steady flow as long as the perturbation wavelength is long compared to the cylinder diameter (Griffin and Hall, 1991). This is confirmed by the good agreement of the synchronization region boundaries in the amplitude–frequency plane for both types of perturbation (Konstantinidis et al., 2003). For in-flow perturbations, a symmetric formation has been reported for circular cylinders (Barbi et al., 1986; Detemple-Laake and Eckelmann, 1989) and a flat plate or T-shaped cylinder (Al-Asmi and Castro, 1992). The symmetric shedding was first observed in oscillatory flow by Barbi et al. (1986) at $f_e/f_o = 1$, but their visualization study did not extend to high-frequency ratios. Detemple-Laake and Eckelmann (1989) photographed an array of five symmetrical vortex pairs (vortex twins) extending several diameters behind the cylinder before these appear to rearrange into a staggered vortex street. Unfortunately, the amplitude of flow forcing (sound waves) was not measured but the frequency of forcing was reported to be near $f_e/f_o \approx 1.5$. Similar results were obtained by Zhou and Graham (2000) in a numerical study of cylinders in large-amplitude oscillatory plus a mean flow. Additionally, their simulations produced the binary vortex street mentioned earlier. The above studies indicate that symmetric shedding can be excited in both laminar and turbulent wake regimes, for bluff bodies with moving as well as fixed separation points.

Symmetric shedding has been associated with self-excited self-sustained streamwise oscillations of compliant cylinders in the so-called first instability region; see, e.g., King et al. (1973), Naudascher (1987), Okajima et al. (2002). Based on kinematic arguments, Naudascher (1987) maintained that this excitation module results from an inward–outward movement of the free shear layers and the ensuing periodic narrowing–widening of the wake synchronized with the cylinder oscillation, termed 'wake and shear-layer breathing'. This module has also been observed in connection with a streamwise only, free oscillation of an elastically supported circular cylinder with two degrees of freedom (Jauvtis and Williamson, 2004). In this study, the freedom of the cylinder to oscillate in the direction of the flow as well as the transverse one, had a drastic effect on the overall vibration response and the vortex wake patterns. The above findings, which demonstrate the significance of streamwise perturbations for the wake patterns and the forces exerted on the body, call for a better understanding of the associated fluid–structure interactions in general and of the symmetric shedding mode in particular.

In the vast majority of previous experimental studies, the identification of the vortex shedding mode was based on flow visualization (Table 1). For both types of forcing, i.e., streamwise cylinder or flow oscillations, there exists a dissimilitude on the conditions for which symmetric shedding takes place. Furthermore, none of the previous studies focused specifically on the symmetric mode of shedding and the associated wake characteristics have not been quantified. Another important question which arises is whether there is a similarity between the symmetric vortex shedding occurring in free and forced oscillations. In view of the above, the present study examines in detail the near wake characteristics of a circular cylinder during symmetric vortex shedding due to periodic flow forcing using quantitative measurement techniques, i.e., laser-Doppler and particle image velocimetry, and the results are discussed in relation to the streamwise free-cylinder oscillations.

2. Experimental details

2.1. Water tunnel

The experimental facility and measurement techniques used for this study were essentially the same as in previous work by the authors (Konstantinidis et al., 2003, 2005a, b). Some details are provided below for completeness. The facility comprises a closed circuit water tunnel with a vertical test-section 72 mm × 72 mm in cross-section and 195 mm long. The test-section is made of transparent plexiglas to allow optical access from all sides. A contraction section of 9:1 area ratio fitted with hexagonal honeycomb and perforated plates precedes the test-section to condition the in-flow. A centrifugal pump delivers flowrates up to $0.3\,m^3$/min and a magnetic flowmeter is used to monitor the bulk flowrate. The temperature of the flowing water is maintained at a constant level by means of a double-jacketed collection chamber and an external cooling/heating unit. The in-flow to the test-section is uniform with a variation of less than 0.5% excluding the boundary layers on the walls, and a background turbulence intensity of 3% in the core (see Fig. 1).

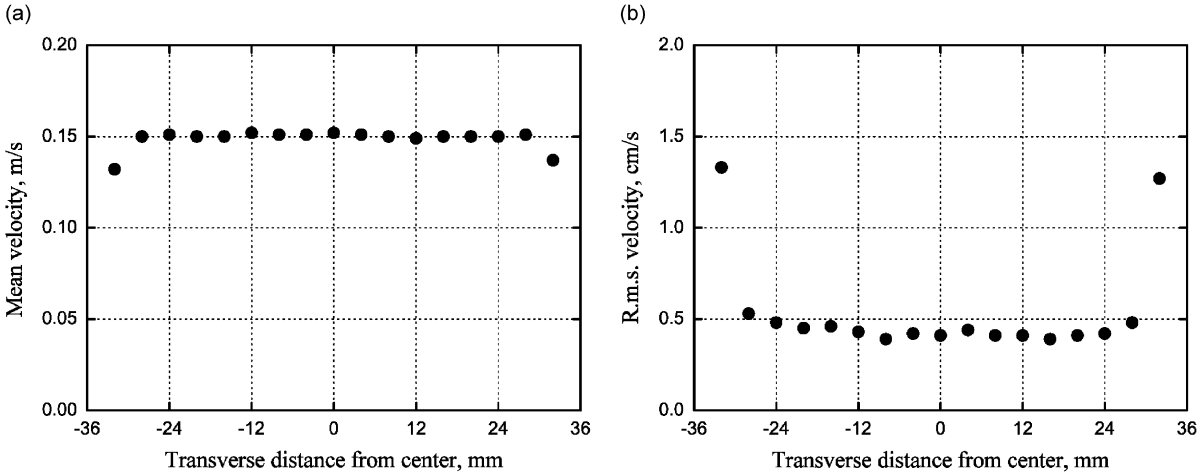

Fig. 1. (a) Profiles of the streamwise mean velocity and (b) its r.m.s. fluctuation measured in the test-section without the model cylinder using LDV. The measurement station is 30 mm below the cylinder position. Statistics were computed from 5000 velocity samples.

A smooth circular cylinder of diameter $D = 7.2$ mm was centrally placed in the test-section and secured on the side walls to eliminate the possibility of vibrations. No end-plates were used. The thickness of the boundary layer developing on the test-section walls at the location of the cylinder is approximately one diameter. Clearly, the boundary layers on the sidewalls interact with the wake giving rise to three-dimensional effects, e.g., oblique vortex shedding and vortex splitting (Williamson, 1996). The present study focuses in the very-near wake patterns at midspan of the cylinder where the above effects do not have a strong influence and are representative of long cylinders. The origin of the coordinate system is located at the centre of the cylinder; x and y denote the streamwise and cross-stream (perpendicular to the cylinder axis) directions, respectively. The corresponding velocity components are u and v.

2.2. Perturbed flow

Flow perturbations were generated by rotating a ball valve which periodically blocked part of the flow passage far upstream of the conditioning and test-sections. Flexible bellows were employed in the flow loop to minimize the transmission of vibrations in the test-section which could not be detected. Unavoidably, the quality of the perturbations is a function of both frequency and flow velocity. The requirement for high perturbation frequencies with respect to the vortex shedding frequency necessitated the use of a relatively lower flow velocity than in previous experiments (Konstantinidis et al., 2003, 2005a, b) in order to produce nearly sinusoidal oscillations of the velocity superimposed onto the mean flow.

The in-flow conditions in the working section were monitored by velocity measurements upstream of the cylinder using laser-Doppler velocimetry (LDV). The same system was employed to measure the wake velocity fluctuations for spectral analysis. A detailed description of the LDV system can be found in Konstantinidis et al. (2003). The in-flow velocity can be approximated as a sinusoidal function of time:

$$U(t) = U_m + \Delta U \sin(2\pi f_e t + \phi), \tag{1}$$

where U_m is the mean in-flow velocity and ΔU is the amplitude of velocity oscillation and ϕ is a reference phase angle relating to the start of the cycle. The phase angle ϕ varies nearly linearly with perturbation frequency and amplitude. The in-flow velocity deviates from the above model equation due to background turbulence introduced by the nature of the tunnel. The r.m.s. deviation between the actual and modelled flow velocity is approximately equal to the background turbulence intensity without flow perturbations (see Fig. 2).

The following dimensionless parameters are employed to describe the flow problem:

$$\text{Reynolds number, } \mathrm{Re} = \frac{\rho U_m D}{\mu}, \tag{2}$$

$$\text{Reduced velocity, } \mathrm{U}^* = \frac{U_m}{f_e D}, \tag{3}$$

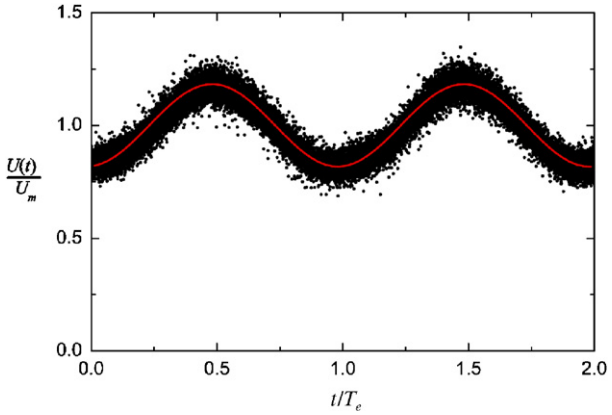

Fig. 2. The in-flow perturbation employed in the experiments is modelled as a sinusoidal oscillation of the velocity. The plot shows the deviation of the instantaneous velocity from the modelled velocity oscillation.

Table 2
Experimental parameters in perturbed flow

Case	1	2	3	4
Reynolds number, Re	1200	1180	1240	1240
Reduced velocity, U*	1.55	1.34	1.23	1.19
Reduced amplitude, A*	0.02	0.04	0.02	0.02
Frequency ratio, f_e/f_o	3.0	3.5	3.8	4.0

$$\text{Reduced amplitude, } A^* = \frac{\Delta U}{2\pi f_e D}, \tag{4}$$

where ρ and μ are the density and the dynamic viscosity of water, respectively. The reduced amplitude is equal to the amplitude of forced streamwise oscillation of a cylinder in a steady approach flow normalized with the cylinder diameter. Another parameter that can be more useful in correlating the data is the frequency ratio f_e/f_o, where f_o is the natural vortex shedding frequency in unforced flow. Here, f_o is computed from a constant Strouhal number relationship $f_o = 0.212U/D$. It should be noted that f_o is based on the frequency of the antisymmetric vortex shedding. Hence, two single vortices are actually shed from alternate sides of the cylinder during one period of vortex shedding. The results reported in this paper were obtained for the conditions shown in Table 2. These cover a range of excitation frequencies from three to four times the unperturbed vortex shedding frequency ($f_e/f_o = 3$–4). In this range, the symmetric vortex shedding mode is predominant (Ongoren and Rockwell, 1988).

2.3. Particle image velocimetry

The wake field was examined using digital particle image velocimetry (PIV). A laser sheet from a 5 W Argon–Ion source illuminated the wake perpendicular to the cylinder axis at midspan. The motion of 10 μm particles inserted in the flow was captured on a CCD camera with a resolution of 1024×1240 pixels. The field of view was approximately $6D$ wide in the cross-stream direction by $7D$ along the streamwise direction. Image pairs were analysed by employing an adaptive cross-correlation methodology. Initially, the images were analysed on fixed 64×64 pixel interrogation windows, followed by analysis on 32×32 pixel windows shifted in the flow direction, for which the PIV settings were optimized. This method produced approximately 4500 velocity vectors in each field excluding the regions covered by the cylinder and its shadow yielding a spatial resolution of $\approx 0.1D$. Further analysis was performed on 16×16 pixel interrogation windows in order to improve the accuracy of the cross-correlation analysis in regions of very steep velocity gradients (Williams et al., 2003). The velocity fields obtained with 32×32 and 16×16 pixel interrogation windows agreed very well and so were the statistical properties of the flow derived from them. Unless otherwise stated,

the vorticity fields shown in this paper were computed from velocity data obtained by using 32×32 pixel interrogation windows which provide a more comprehensible view of the flow. All images were phase-referenced with respect to the phase of the in-flow oscillation. Phase information was provided by a high-precision optical encoder attached to the shaft of the perturbation-generating rotating valve. Velocity gradients were computed employing a least-squares formula in order to produce smooth distributions of vorticity $\zeta = \partial v/\partial x - \partial u/\partial y$ (Raffel et al., 1998). Vorticity values are normalized with the cylinder diameter and flow velocity, i.e., $\zeta D/U$.

3. Results and discussion

3.1. Preliminary tests in unperturbed flow

Preliminary measurements were carried out to examine the cylinder wake without in-flow perturbations for reference purposes. Some important wake parameters such as the Strouhal number, the recirculation bubble length, the vortex formation region, and the drag coefficient were estimated from these measurements and the results are summarized in Table 3. The wake frequency was estimated from spectra of the velocity fluctuations in the separating shear layer (see Fig. 3). A peak at the natural vortex shedding frequency f_o is observed without any harmonics thereof. The corresponding Strouhal number ($\mathrm{St} = f_o D/U$) is in agreement with the compiled data reported in Norberg (2003). The recirculation bubble is the extent of the reversed flow region in the base of the cylinder, marked by the location of zero mean velocity along the wake centreline. The vortex formation region is customarily defined by the location of maximum intensity fluctuations of the streamwise u-component along the wake centreline (Griffin, 1995). These length scales are measured from the centre of the cylinder. The corresponding values in Table 3 compare well with those reported in Norberg (1998) in spite of the differences in the disturbance levels of the ambient flow, aspect ratio and blockage effects. The limited sensitivity to these influencing parameters in this Re range was also observed in the previous LDV measurements (Konstantinidis et al., 2003).

The average drag coefficient was estimated from the wake profiles of the mean velocity and Reynolds stresses using the formula suggested by Antonia and Rajagopalan (1990):

$$C_D = 2\int_{-\infty}^{\infty} \frac{\bar{U}}{U_e}\left(\frac{U_e - \bar{U}}{U_e}\right)\mathrm{d}\left(\frac{y}{D}\right) + 2\int_{-\infty}^{\infty}\left(\frac{\overline{v^2} - \overline{u^2}}{U_e^2}\right)\mathrm{d}\left(\frac{y}{D}\right), \tag{5}$$

where $\bar{U}$ is the local mean velocity, U_e is the external velocity of undisturbed flow and $\overline{u^2}$ and $\overline{v^2}$ are the streamwise and cross-stream Reynolds stresses. The above formula yields approximately constant values when applied in the region $x/D > 3.5$ where there are no overshoots in the mean velocity profiles. The computed drag coefficient is only slightly higher than expected from the published literature (Bishop and Hassan, 1964; Zdravkovich, 1997). Taking into account the 10% blockage in the present study, the C_D estimate may be considered reasonably accurate. The same method is employed later on to estimate the drag from phase-averaged wake measurements.

The long vortex formation region found in the present study (Table 3) corresponds to a Re range of weak vortex shedding activity in which the shear-layer instability plays an important role (Norberg, 2003). Fig. 4 shows typical instantaneous patterns of vorticity distribution in the wake in terms of contour lines and coloured floods. The contour lines correspond to PIV analysis with 32×32 pixels interrogation windows and the contoured floods to 16×16 pixels. The thin shear layers emanating from the cylinder are parallel at first and the so-called 'Bloor–Gerrard' vortices develop therein (Fig. 4(a)). Large-scale vorticity is concentrated downstream, giving rise to the familiar antisymmetric or alternating vortex shedding. However, large-scale vortices may form close to the base of the cylinder as in Fig. 4(b). These two patterns are comparable to the 'high-quality' and 'low-quality' shedding modes, respectively, inferred by Norberg (2003). The co-existence of these two modes at such low Re might be attributed to the influence of background

Table 3
Summary of wake characteristics in unperturbed flow

Reynolds number, Re	$1070 \pm 1.6\%$
Strouhal number, St	$0.212 \pm 2.7\%$
Recirculation bubble length, l_b	$2.19D \pm 1.5\%$
Vortex formation length, l_f	$2.3D \pm 5.0\%$
Drag coefficient, C_D	$1.13 \pm 6.2\%$

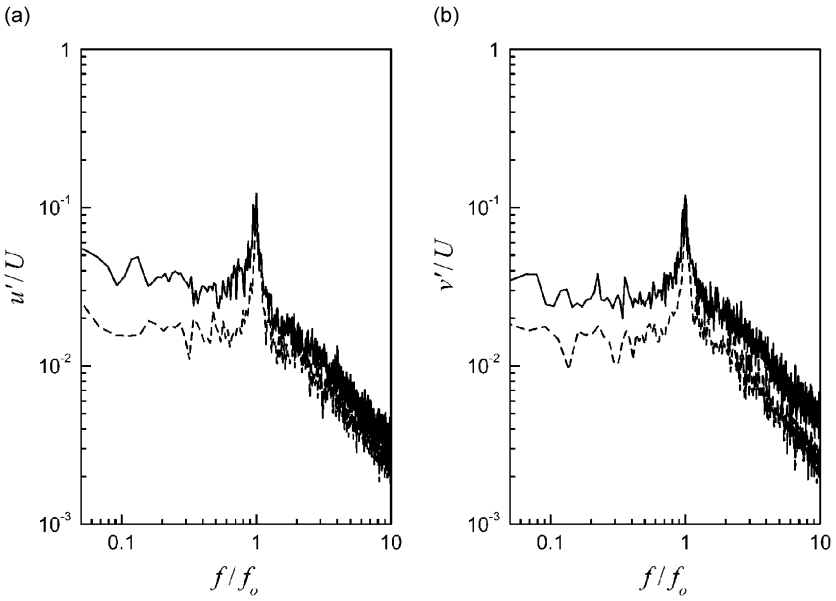

Fig. 3. Spectra of the velocity fluctuations in the unperturbed wake: (a) streamwise component and (b) cross-stream component; $Re \approx 1000$. Measurements obtained at $\{x/D, y/D\} = \{2, 0.5\}$ (solid lines) and $\{x/D, y/D\} = \{3, 1\}$ (broken lines).

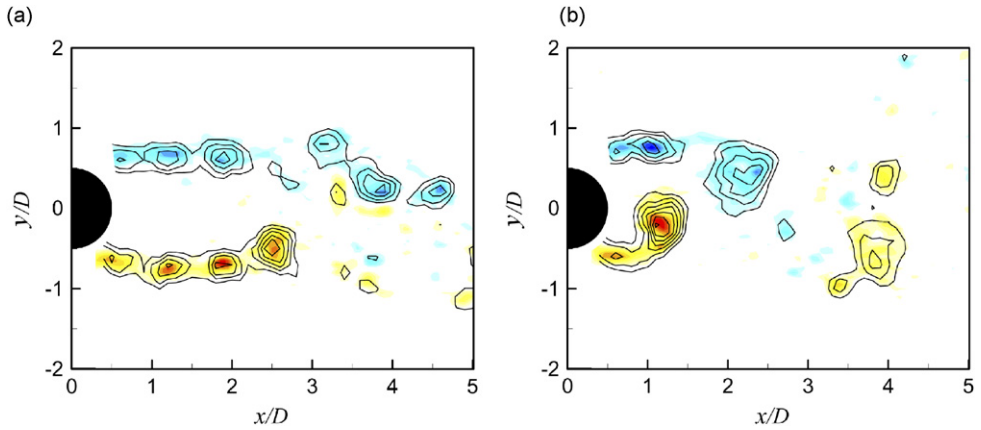

Fig. 4. Instantaneous patterns of vorticity distribution in the cylinder wake for unperturbed flow. $Re = 1070$. Vorticity contours $\zeta D/U = \pm 1 \pm 2, \pm 3 \ldots$.

turbulence which promotes the transition in the shear layers. The vorticity patterns are similar at both resolutions, though the contour lines represent a spatially filtered distribution. This suggests that even the measurements at the lower resolution represent the instantaneous flow characteristics properly. In the following, only the results obtained with the lower resolution (32×32 pixels) are shown.

The role of the shear-layer or Bloor–Gerrard vortices in the development of cylinder wakes has received considerable attention, e.g., see Prasad and Williamson (1997), Rajagopalan and Antonia (2005) and the references cited therein. It has been suggested that the initiation of shear-layer vortices occurs at $Re = 750$ for a cylinder without end-plates and it may occur at even lower Re when the ambient flow is noisy. Therefore, the occurrence of well-established shear-layer vortices in the present study is not surprising. Rajagopalan and Antonia (2005) suggested a relationship $f_{sl}/f_w = 0.029Re^{0.65}$ for predicting the frequency of the shear-layer vortices f_{sl} where f_w is the frequency of large-scale vortex shedding in the wake. This relationship gives $f_{sl}/f_w = 2.7$ at $Re = 1070$ of the present unperturbed flow experiment. A rough estimate of the shear-layer frequency from the present data ranges between $f_{sl}/f_w \approx 3$–4. Interestingly, the frequency of the imposed flow perturbations f_e employed in the present experiments (see next section) is in the same

range. Therefore, the possibility of interaction between the shear-layer and forcing frequencies, which implies that the results of this study might depend on the Reynolds number, should be taken into account.

3.2. Overview of vortex patterns in perturbed flow

This section describes the vortex patterns in the cylinder wake when the in-flow velocity has periodic oscillations superimposed on the mean. In the following, the case number or the frequency ratio will be invoked to refer to the experimental parameters of Table 2.

Over the range of perturbation frequencies employed, a symmetric mode of vortex formation predominates close to the cylinder where vortices form on both sides of the cylinder simultaneously (vortex twins or pairs). Further downstream, the symmetric vortices become gradually asymmetric and rearrange into a staggered vortex street, more appropriately characterized as a wavering motion of the vortex structures. The location where the symmetry of the wake breaks down varies during any single experiment. Examination of a large number of vorticity fields shows that the location of symmetry breaking is a probabilistic function of both the frequency ratio and the reduced amplitude. Typical examples of the instantaneous wake patterns in perturbed flow are shown in Figs. 5 and 6 for $f_e/f_o = 3$ and 4, respectively. The instances correspond to the timing of maximum flow velocity in the oscillation cycle to facilitate comparison.

Fig. 5(a) shows a symmetric arrangement of two vortex pairs in the near wake of the cylinder and a gradual transition to an asymmetric pattern further downstream. Up to three symmetric vortex pairs have been observed in the near wake. However, the loss of symmetry may occur closer to the cylinder as in Fig. 5(b) where the wake becomes asymmetric immediately after the initial formation of symmetric vortices on both sides of the cylinder.

Fig. 6(a) and (b) show the corresponding symmetric and antisymmetric vortex patterns for $f_e/f_o = 4$. Similar patterns were observed in all test cases but, quantitatively, the probability of their occurrence was a function of the perturbation parameters.

In order to quantify the observations, the vorticity distributions were cast into four groups. A vortex pattern is designated SS3 indicating three symmetric vortex pairs in the near wake. Analogously, SS2 and SS1 designate two and one symmetric vortex pairs before the wake becomes asymmetric. The shedding of vorticity in a predominantly antisymmetric mode is designated AS. Fig. 7 shows the probability of occurrence of the different vortex patterns obtained by visual inspection of at least 60 instantaneous vorticity fields in each case. The results show that the wake symmetry is sustained farther at $f_e/f_o = 3$ (case 1) than it is at $f_e/f_o = 4$ (case 4) for approximately the same perturbation amplitude. However, the trend is not monotonic as symmetry breaking is observed closest to the cylinder at $f_e/f_o = 3.8$. The SS3 vortex pattern is most notably observed for case 2 that corresponds to relatively higher perturbation amplitude than the other cases. A strong competition between the antisymmetric and symmetric modes of shedding is observed in cases 3 and 4. These results suggest that the effect of perturbations is a complex function of both the amplitude and frequency of flow forcing even in the relatively narrow range $f_e/f_o = 3$–4. Ongoren and Rockwell (1988) have noted only the symmetric vortex shedding over the same range. However, the field of view in their experiments extended to about three diameters from the centre of the cylinder. This implies that symmetry breaking in the downstream wake could not

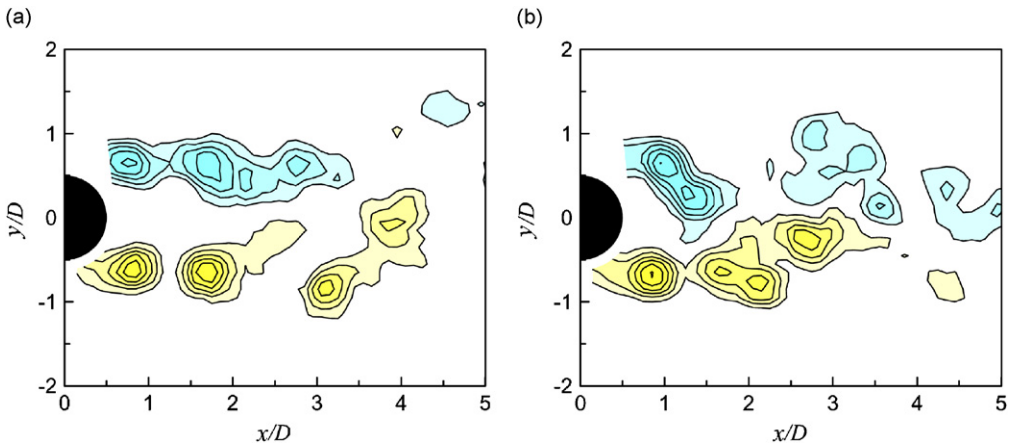

Fig. 5. Instantaneous patterns of vorticity distribution in the cylinder wake for perturbed flow; $f_e/f_o = 3$. The patterns correspond to the phase of maximum in-flow velocity. Contour levels: $\zeta D/U = \pm 1, \pm 2 \ldots$.

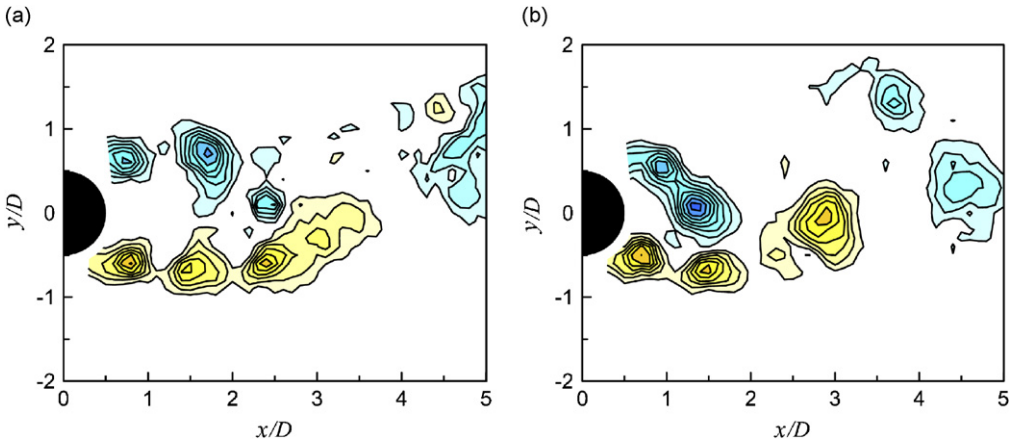

Fig. 6. Instantaneous patterns of vorticity distribution in the cylinder wake for perturbed flow; $f_e/f_o = 4$. The patterns correspond to the phase of maximum in-flow velocity. Contour levels: $\zeta D/U = \pm 1, \pm 2 \ldots$.

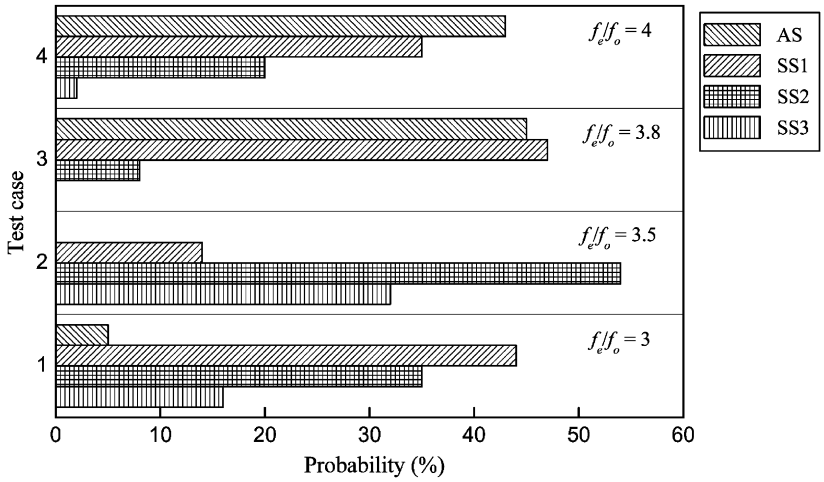

Fig. 7. Probability of occurrence of vortex patterns.

be observed, if present. Given the relatively high amplitude of cylinder oscillation employed in their experiments ($A^* = 0.13$), it is not surprising that only the symmetric mode was observed in the wake. It is reasonable to expect that the persistence of the wake symmetry may increase with increasing forcing amplitude since the induced perturbation is purely symmetric. It is very interesting to note though that increasing the forcing amplitude within the fundamental lock-on range ($f_e/f_o \approx 2$) results in an enhancement of the antisymmetric mode (Konstantinidis and Balabani, 2006).

The initial formation of the symmetric vortices on the two sides of the cylinder is essentially phase-locked to the cyclic variation of the flow velocity, i.e., they appear repeatedly at nearly the same location from one cycle to the next, as can be verified in Figs. 5 and 6. This allows averaging of the instantaneous vorticity fields at constant phase with respect to the flow oscillation. Fig. 8 shows the phase-averaged distributions of vorticity $\langle\zeta\rangle$ in the near wake for all cases examined (the brackets denote phase-averaging). Each distribution corresponds to the timing of maximum in-flow velocity. The distributions exemplify the results of Fig. 7. The lack of appreciable vorticity in the downstream region is indicative of the average location where symmetry breaking occurs, i.e., the fluctuations associated with vortex shedding are random in phase beyond this location as opposed to the repeatable formation of symmetric vortices close to the cylinder.

Fig. 9 shows the difference between the phase-averaged and time-averaged vorticity distributions, $\tilde{\zeta} = \langle\zeta\rangle - \bar{\zeta}$ where the overbar denotes a time average. The existence of phase-locked vortices causes substantial deviations from the vorticity distribution associated with the mean flow. It is worth noting that fluid from the outer flow is strongly sucked

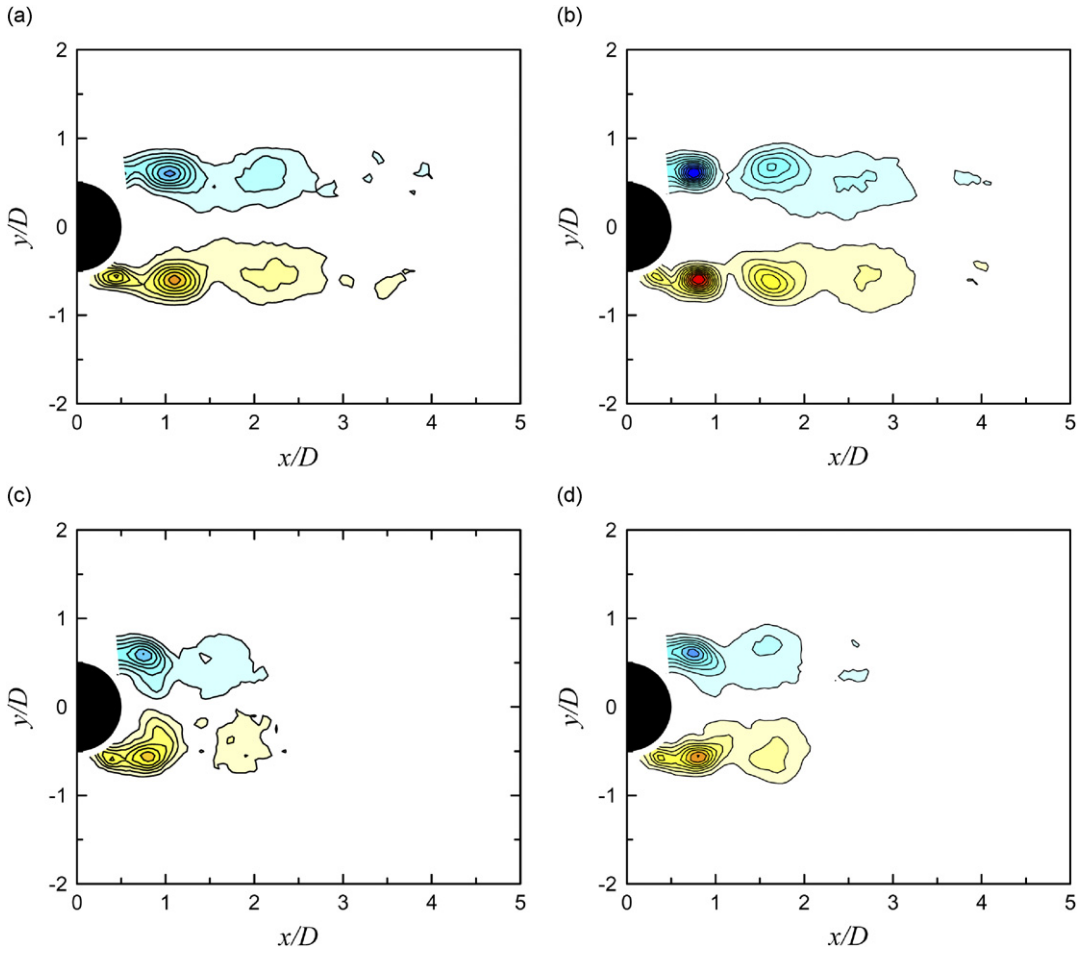

Fig. 8. Phase-averaged patterns of vorticity distribution in perturbed flow: (a) $f_e/f_o = 3$, (b) $f_e/f_o = 3.5$, (c) $f_e/f_o = 3.8$, (d) $f_e/f_o = 4$. The patterns correspond to the phase of maximum in-flow velocity in each case. Contour levels: $\langle\zeta\rangle D/U = \pm 1, \pm 2 \ldots$.

in-between the shed vortex pairs producing characteristic deviations in the sign of the fluctuating vorticity, most markedly seen in Fig. 9(b). The differences in the vorticity distributions among the cases examined clearly attest that the wake kinematics are strongly affected by the flow perturbations.

3.3. Wake spectra

The velocity fluctuations in the near wake were measured with LDV and the dominant frequencies were identified by spectral analysis. Fig. 10 shows the spectra of the streamwise velocity fluctuations obtained in the separating shear layer $\{x/D, y/D\} = \{2, 0.5\}$ for all experimental cases. The spectra for $f_e/f_o = 3$ (case 1) in Fig. 10(a) display a distinct peak at the perturbation frequency f_e, a pronounced peak at a frequency f_w, approximately equal to the natural shedding frequency, i.e., $f_w \approx f_o$, and a less marked peak at the frequency $f_d = f_e - f_w$. A plausible interpretation of the spectra is that f_w is associated with the reconstruction of the wake at the antisymmetric mode. This entails coalescence and/or annihilation of vorticity shed from either side of the cylinder during three consecutive oscillation cycles to form two alternating vortices downstream. This merging process is complicated by turbulent mixing and diffusion as was observed in the instantaneous distributions of vorticity. The peak at f_d results from the nonlinear interaction between f_e and f_w. Similar nonlinear interactions have been observed in cylinder arrays in cross-flow where the shedding of vorticity occurs at different frequencies from the first and the inner rows (Oengören and Ziada, 1998). It emerges when the interacting frequency components are comparably strong, as in the present case. Similar spectral characteristics are observed for $f_e/f_o = 3.5$ in Fig. 10(b).

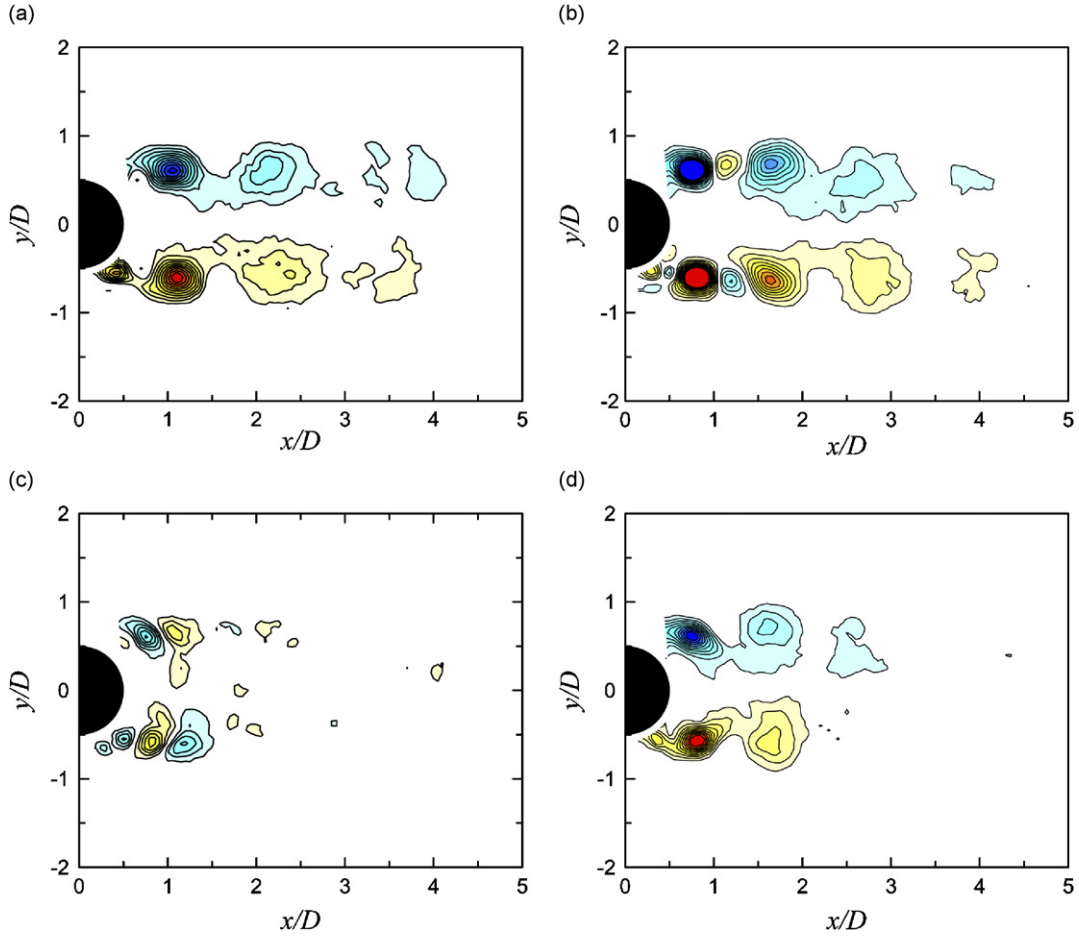

Fig. 9. Phase-averaged patterns of fluctuating vorticity distribution in perturbed flow: (a) $f_e/f_o = 3$, (b) $f_e/f_o = 3.5$, (c) $f_e/f_o = 3.8$, (d) $f_e/f_o = 4$. The patterns correspond to the phase of maximum in-flow velocity in each case. Contour levels: $\tilde{\zeta}D/U = \pm 0.5, \pm 1 \ldots$.

For the perturbation frequencies $f_e/f_o = 3.8$ and 4, the wake frequency 'locks on' to the $f_e/4$ sub-harmonic (Fig. 10(c–d)). The phase-locking of the fluctuations at f_w and f_e manifests itself by the amplification of the f_w peak and the emergence of multiple harmonics of the perturbation frequency in the spectra. Evidence of such 'secondary' lock-on was also observed by Barbi et al. (1986) in oscillatory flow around a stationary cylinder. The instantaneous patterns reveal a strong competition between symmetric and antisymmetric vortex shedding both of which are phase-locked. When symmetric shedding occurs in the near wake, eight vortices shed from either side of the cylinder during four consecutive cycles, coalesce to form two antisymmetric vortices downstream as in Fig. 6(a); therefore, the vortex shedding frequency can be as high as four times the shedding frequency of the stationary cylinder. However, in the antisymmetric mode, the individual vortices tend to retain their integrity and form an alternating pattern of vortex couples downstream as in Fig. 6(b). This pattern resembles the 2P mode observed in the wake of a cylinder oscillating in the cross-stream direction (Williamson and Roshko, 1988). In the present case, however, the formation of the vortex pair occurs in distinct cycles of oscillation.

The spectral characteristics of the velocity fluctuations are strongly dependent on the measurement location. As an example, Fig. 11 shows the spectra of both the streamwise and cross-stream velocity fluctuations at two different locations for case 1 ($f_e/f_o = 3$). In the wake centreline, the spectra of the streamwise velocity exhibit a distinct peak at f_e together with hardly distinguished peaks at f_w and f_d (Fig. 11(a)). The dominance of the f_e component is probably induced by the periodic ejections of fluid from the upstream symmetric wake. Off the centreline $\{x/D, y/D\} = \{3, 1\}$, the peak at f_w is more distinct. However, the spectra of the cross-stream component are dominated by the fluctuations at f_w at both measurement locations (Fig. 11(b)). These results provide a consistent understanding of the vortex shedding and

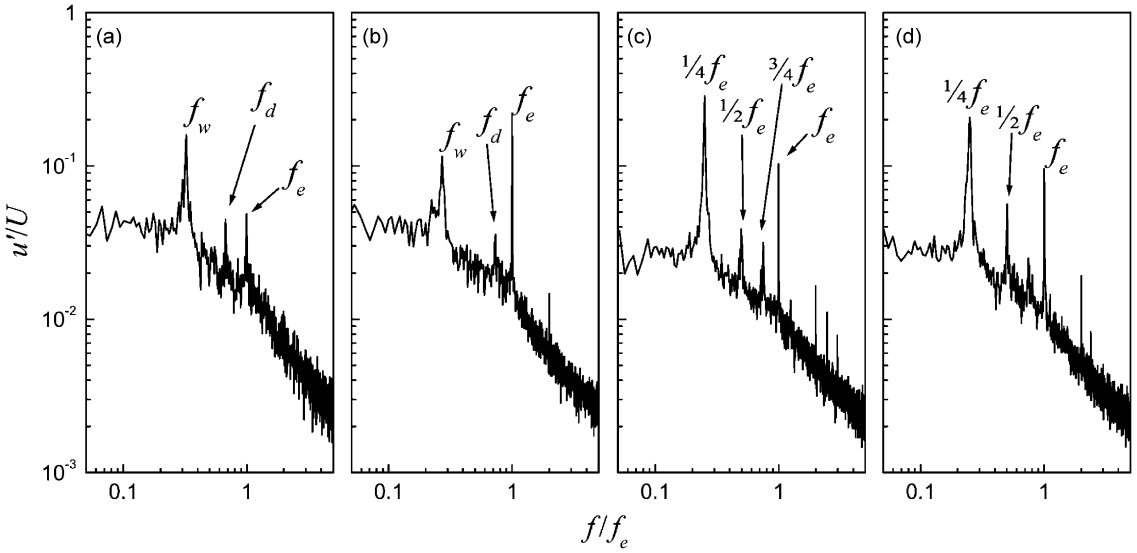

Fig. 10. Spectra of the streamwise velocity fluctuations at $\{x/D, y/D\} = \{2, 0.5\}$ in perturbed flow. (a) $f_e/f_o = 3$, (b) $f_e/f_o = 3.5$, (c) $f_e/f_o = 3.8$, (d) $f_e/f_o = 4$.

downstream wake frequencies and call for particular attention in interpreting spectral characteristics which can be a source of errors.

3.4. Wake breathing, fluctuating drag and flow-induced vibrations

The formation and shedding of symmetric vortices has been recognized as a source of flow-induced streamwise oscillations of compliant cylinders by several investigators (Hardwick and Wootton, 1973; King et al., 1973; King, 1977; Naudascher, 1987; Okajima et al., 2002; Jauvtis and Williamson, 2004). Naudascher maintained that the excitation force results from an inward–outward movement of the free shear layers and the ensuing periodic narrowing–widening of the wake synchronized with the cylinder oscillation. He termed this excitation module 'wake and shear-layer breathing'. He then developed an equation to predict the conditions of self-limitation of vibration on the assumption that the fluid-dynamic force is in-phase with the cylinder velocity. However, the energy transfer between the fluid and the structure is dependent on the actual phasing between the exciting force and the resulting motion and associated feedback effects. In this respect, it is interesting to examine the wake kinematics and the resulting fluctuating drag force in relation to the phase of flow oscillation, or the equivalent streamwise motion of a cylinder relative to a steady flow.

To draw a comparison between forced and self-excited (or free) oscillations, Fig. 12 shows streak-line patterns at four instances during a cycle of oscillation for both cases. Fig. 12(a) shows the patterns obtained in the present forced flow experiments (phase-averaged data obtained for $f_e/f_o = 3$) while the analogous patterns in self-excited oscillations are conceptually reproduced in Fig. 12(b) after Naudascher (1987). Fig. 12(c) shows the relative velocity between the flow and the cylinder, $U(t) = U_m - \dot{x}_c(t)$, where $\dot{x}_c(t)$ is the velocity of an oscillating cylinder in time-steady flow, at the corresponding instants during the cycle. Apparently, $U(t)$ is equal to the time-dependent flow velocity in the present forced flow oscillations around a stationary cylinder. At time $t/T_e = 0.1$, the velocity of the cylinder is zero, i.e., $-\dot{x}_c = U(t) - U_m = 0$, corresponding to the most downstream position of the cylinder. At this instant, twin vortices are attached to the rear of the cylinder. As the cylinder moves upstream, the flow accelerates relative to the cylinder and the symmetric vortices are pushed away and shed from the cylinder ($t/T_e = 0.35$). This shedding of vorticity in the wake impulses a thrust force on the cylinder (it should be noted that the net circulation of the vortex pair is zero for perfectly symmetric vortices). By the time the cylinder reaches its furthest upstream position at $t/T_e = 0.6$, the shed vortices have enough momentum to be convected downstream in the decelerating flow. According to Naudascher (1987), a new vortex pair starts to grow near the separation points at the same time (not resolved by the present measurements). As the cylinder moves downstream through its mid-position, the relative velocity takes its minimum value and the new vortices grow symmetrically on the sides of the cylinder ($t/T_e = 0.85$). The vortex pair remains attached to the cylinder surface until the cylinder reverses direction and the flow starts to accelerate relative to the cylinder. This completes a full cycle of oscillation. It can be argued that, while the twin vortices remain attached to the cylinder, i.e., during its

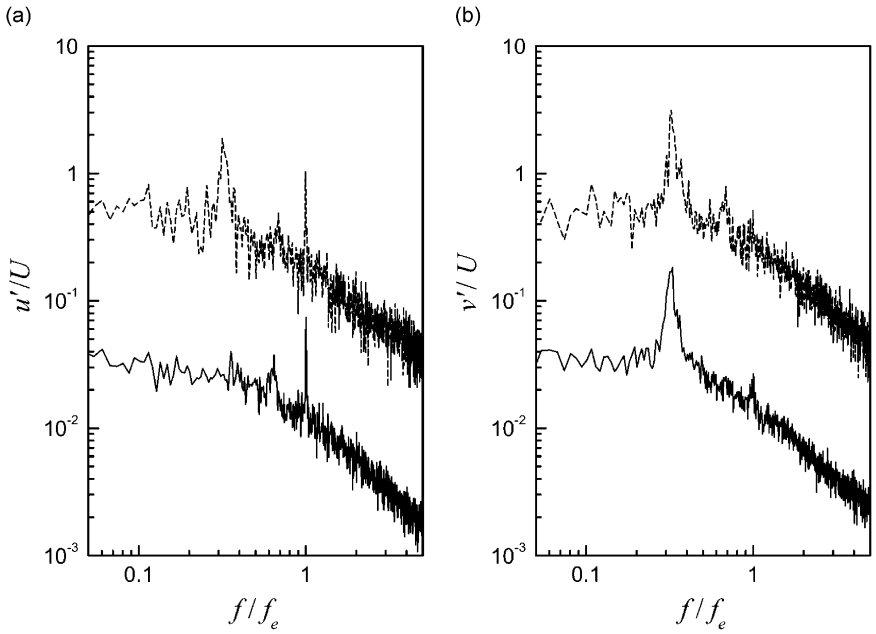

Fig. 11. (a) Spectra of the steamwise and (b) cross-stream velocity fluctuations at $x/D = 3$; $f_e/f_o = 3.5$. $y/D = 0$ (solid line), $y/D = 1$ (broken line). Broken lines are displaced vertically for clarity.

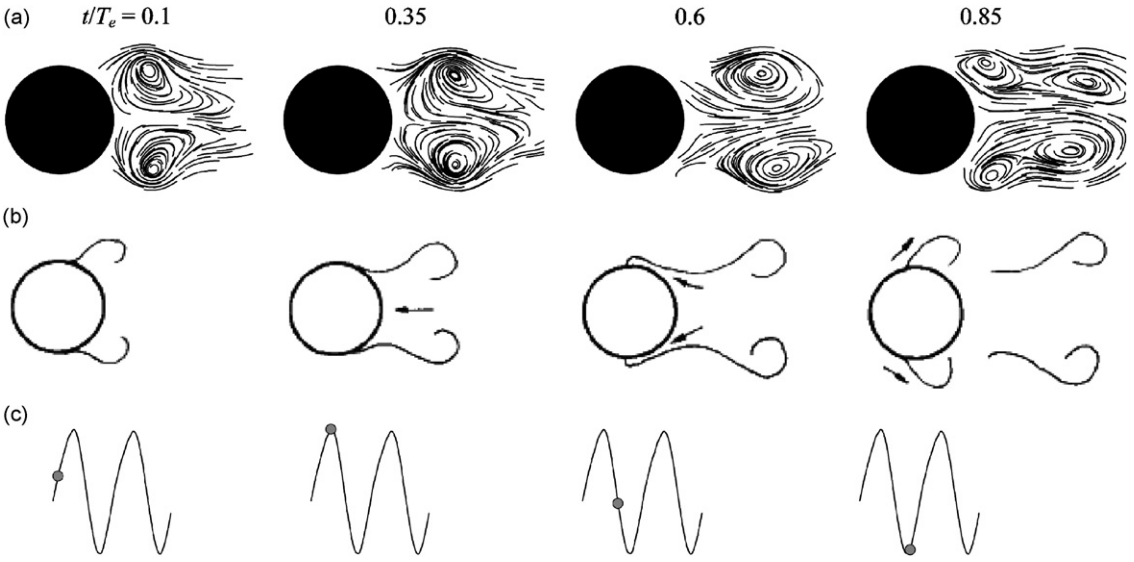

Fig. 12. (a) Phase-averaged streak-line patterns in the perturbed wake ($f_e/f_o = 3$). (b) Wake patterns occurring in streamwise flow-induced vibration [after Naudascher (1987)]. (c) Flow velocity relative to stationary cylinder for both (a) and (b).

downstream motion ($t/T_e = 0.6$–0.85), the projected area normal to the flow of a virtual body comprising the cylinder and the attached fluid mass increases and thereby the drag coefficient is effectively increased. This effect, which is conceded by the variation of the fluctuating drag given further below, might be linked to variations of the 'added mass' during a cycle (Naudascher, 1987; Sarpkaya, 2004). Such an interpretation would justify Sarpkaya's assertion that it is impossible to separate an inertial force that comprises added mass from the total force experienced by the cylinder since the added-mass effect is caused by the redistribution of the flow from motion-induced vortices in this particular case.

The phasing of the wake kinematics with respect to the cylinder motion exhibits remarkable similarity between forced and free oscillations. It therefore appears possible to relate the forced oscillation data to the response of a freely vibrating cylinder in the first instability region which has been associated with symmetric vortex shedding. The drag coefficient at each phase of the flow oscillation can be estimated using a quasi-steady approach with the aid of Eq. (5). This is reasonable, given the fact that the wake downstream the location of symmetry breaking is not phase-locked to the flow oscillation (for $f_e/f_o = 3$ and 3.5 only). Therefore, the phase-averaged velocity statistics in the downstream region are the same as the time-averaged statistics of a virtual bluff-body in steady flow. By virtue of the quasi-steady approach adopted here, the external flow velocity $U_e(t) \approx U_m - \dot{x}_c(t)$ is employed in Eq. (5) and the estimated drag coefficient is

$$C_D(t) = \frac{F_D(t)}{\frac{1}{2}\rho U_e^2 A_p} = \frac{F_D(t)}{\frac{1}{2}\rho U_m^2 A_p \left[1 - \frac{\dot{x}_c(t)}{U_m}\right]^2}, \tag{6}$$

where $F_D(t)$ is the unsteady drag force and A_p is the projected area of the cylinder normal to the flow ($= LD$, where L is the length of the cylinder). Applying Eq. (6) to the phase-averaged data for each of the four available phases shown in Fig. 12 yields the variation of the unsteady drag coefficient $C_D(t)$ which is shown together with $\dot{x}_c(t)$ in Fig. 13. Thus, the computed drag coefficient [symbols in Fig. 13(b)] did not vary considerably at different stations along the wake as indicated by the error bars, and therefore the estimates are deemed reasonably accurate. The mean drag coefficient in perturbed flow is 1.15 at $f_e/f_o = 3$ which is close to 1.13 found in unperturbed flow (see Table 3). These results agree well with the directly measured values of Nishihara et al. (2005) for both stationary and oscillating cylinders, although comparisons should be made cautiously due to differences in Reynolds number, dimensionless amplitude of oscillation and experimental configuration. They have measured a mean drag coefficient of 1.10 for steady flow ($\mathrm{Re} = 1.7 \times 10^4$) and 1.16 for a cylinder oscillating at $f_e/f_o = 3$ ($\mathrm{A}^* = 0.05$). It should be noted that the reduced velocity is dependent on the Strouhal number for a given frequency ratio, i.e., $\mathrm{U}^* = (f_e/f_o)^{-1}\mathrm{St}^{-1} = 1.81$ in their experiment, corresponding to 1.55 in the present study.

In flow-induced streamwise vibrations, the excitation force is the fluctuating drag since the mean drag cannot do positive work on the body. Naudascher (1987) attributed the fluctuating drag to the breathing motion of the wake and the shear layers which accompanies the motion of the cylinder *vis-à-vis* flow. Irrespective of the fluid-dynamic origin, by expressing the drag coefficient in terms of mean and fluctuating components $C_D(t) = \bar{C}_D + C'_D(t)$, then the excitation force $F_e(t)$ is simply the fluctuating part:

$$F_e(t) = \frac{1}{2}\rho U_m^2 A_p C'_D(t). \tag{7}$$

It should be pointed out that the formulation of $C'_D(t)$ in Eq. (7) incorporates fluid damping (negative excitation) due to the mean drag force arising from changes in relative velocity by virtue of Eq. (6) [see Naudascher (1987)] but excludes the inertial force that would have been measured with strain gauges in the laboratory. However, the inertial force is conservative and does not have any influence on the analysis presented here. The work done by the excitation force during a cycle of oscillation is given by

$$W_e = \oint F_e(t)\,\mathrm{d}x_c = \int_0^T F_e(t)\dot{x}_c(t)\,\mathrm{d}t, \tag{8}$$

where $x_c(t)$ is the streamwise position of the cylinder ($x_c = 0$ with no oscillation). Following the work of Blackburn and Henderson (1999) and Jauvtis and Williamson (2004), the dimensionless rate of energy transfer $\dot{e}(t)$ and the coefficient of energy transfer C_E between the fluid and the structure are defined as

$$C_E = \int_0^1 C'_D(t)\left[\frac{\dot{x}_c(t)}{U_m}\right]\mathrm{d}\left(\frac{t}{T_e}\right) = \int_0^1 \dot{e}(t^*)\,\mathrm{d}(t^*). \tag{9}$$

Whether $F_e(t)$ excites or damps the streamwise vibration depends on its phasing with respect to $x_c(t)$. If the oscillation of the cylinder and the fluctuating drag were sinusoidal, it can be readily shown that the phase difference between $F_e(t)$ and $x_c(t)$ must be positive for energy transfer from the fluid to the structure, e.g., see Carberry et al. (2005) for the corresponding scenario in transverse oscillations. However, neither $x_c(t)$ nor $F_e(t)$ need to be sinusoidal and the criterion for self-excited vibrations is that C_E must be positive.

The rate of energy transfer can be computed from the known variations of $\dot{x}_c(t)$ and $C'_D(t)$ during a cycle. Since the variation of the fluctuating drag could be estimated at only four phases, a cubic-spline with periodic end conditions was fitted to the data shown as a solid line in Fig. 13(b). A broken line indicates a sine function which is not as good a fit to the $C'_D(t)$ data, though the difference to the spline fit is within the experimental uncertainty of the data. The resulting

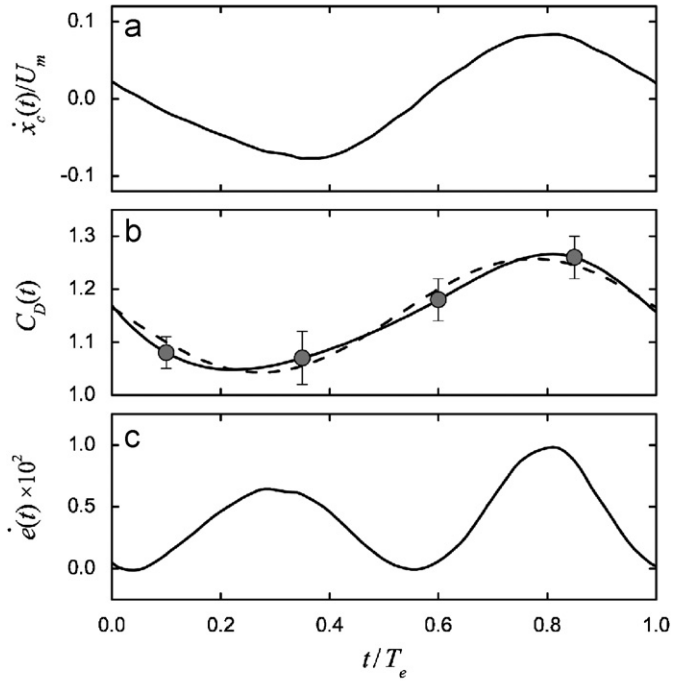

Fig. 13. Cylinder velocity relative to steady flow $\dot{x}_c(t)$, unsteady drag coefficient $C_D(t)$, and the rate of energy transfer between the fluid and structure $\dot{e}(t)$ during a cycle of oscillation ($f_e/f_o = 3$).

variation of $\dot{e}(t)$ is shown in Fig. 13(c). The importance of Fig. 13 is that the fluctuating drag $C'_D(t)$ is almost in phase with $\dot{x}_c(t)$. This implies that energy is transferred from the fluid to the structure or, in other words, that the fluctuating drag does positive work on a freely oscillating structure ($C_E > 0$). The rate of energy transfer is positive almost during the complete cycle, which corresponds to maximum energy transfer (Fig. 13(c)). More positive work is done during flow deceleration relative to the cylinder (cylinder moving downstream) due to a drag overshoot (associated with the increase in the projected area of the virtual body as discussed earlier) than during flow acceleration. The above findings agree qualitatively with the direct measurements of Nishihara et al. (2005). Direct comparisons of the fluctuating drag and its phase with respect to cylinder motion are not possible because their measurements by strain gauges include inertial effects. Their results show that the unsteady drag force acts as an excitation while the added damping is negative for perturbation frequencies near $f_e/f_o = 3$ (corresponding to a reduced velocity $U^* = 1.81$). This provides further verification for the present results and confidence that the arguments put forward can explain how symmetric shedding can excite free oscillations of compliant cylinders in the so-called first instability region (King, 1977; Okajima et al., 2002). It should be emphasized that this excitation module is not active in the absence of streamwise perturbations, i.e., when appropriate conditions for symmetric vortex shedding do not exist.

4. Conclusions

Experiments were carried out to study the wake of a circular cylinder during symmetric vortex shedding. The in-flow was perturbed by a periodic oscillation imposed on flow velocity at frequencies between three and four times the natural shedding frequency in order to promote the symmetric mode of vortex shedding. The results obtained for Reynolds numbers about 1200 are similar to those known for streamwise oscillations of the cylinder in a time-steady flow. The most important findings can be summarized as follows.

(a) The symmetric arrangement of twin vortices in the very-near wake is not stable and always gives way to an antisymmetric pattern further downstream, at least for small perturbation amplitudes. The occurrence of the symmetric mode and the number of cycles for which the symmetric arrangement persists are probabilistic functions

of the perturbation frequency and amplitude but the interaction between symmetric and antisymmetric modes is complex.

(b) The initial formation of symmetric vortices on both sides of the cylinder is always phase-locked to the flow/cylinder oscillation, i.e., it is a direct consequence of the imposed symmetric perturbation.

(c) The frequency of large-scale antisymmetric vortices in the downstream wake may be synchronized or not to the imposed flow/cylinder oscillation and is close to that of the stationary cylinder even though the symmetric vortex shedding frequency can be as high as four times that of the stationary cylinder.

(d) There is a close correspondence of the wake kinematics and their phasing between forced and flow-induced streamwise oscillations for perturbation frequencies near three times the natural shedding frequency of the unperturbed wake.

(e) The symmetric shedding of vortices very close to the cylinder produces a synchronized movement of the wake (shear layer and wake breathing). This induces a fluctuating drag force in-phase with the relative flow/cylinder velocity acting on the structure which is associated with positive energy transfer from the fluid to the structure.

The present study provides insight into the wake characteristics associated with symmetric vortex shedding from a circular cylinder due to fluid–structure interactions and consolidates previous related observations, often unaccounted for, found in the published literature.

Acknowledgement

Financial support for conducting the experiments reported in this paper was provided by EPSRC.

References

Al-Asmi, K., Castro, P., 1992. Vortex shedding in oscillatory flow: geometrical effects. Flow Measurement and Instrumentation 3, 187–202.

Antonia, R.A., Rajagopalan, S., 1990. Determination of drag of a circular cylinder. AIAA Journal 28, 1833–1834.

Barbi, C., Favier, D.P., Maresca, C.A., Telionis, D.P., 1986. Vortex shedding and lock-on of a circular cylinder in oscillatory flow. Journal of Fluid Mechanics 170, 527–544.

Bishop, R.E.D., Hassan, A.Y., 1964. The lift and drag forces on a circular cylinder in a flowing fluid. Proceedings of the Royal Society of London, Series A, Mathematical and Physical Sciences 277 (1368), 32–50.

Blackburn, H.M., Henderson, R.D., 1999. A study of two-dimensional flow past an oscillating cylinder. Journal of Fluid Mechanics 385, 255–286.

Carberry, J., Sheridan, J., Rockwell, D., 2005. Controlled oscillations of a cylinder: forces and wake modes. Journal of Fluid Mechanics 538, 31–69.

Cetiner, O., Rockwell, D., 2001. Streamwise oscillations of a cylinder in a steady current. Part 1. Locked-on states of vortex formation and loading. Journal of Fluid Mechanics 427, 1–28.

Detemple-Laake, E., Eckelmann, H., 1989. Phenomenology of Kármán vortex streets in oscillatory flow. Experiments in Fluids 7, 217–227.

Gau, C., Wu, S.X., Su, H.S., 2001. Synchronization of vortex shedding and heat transfer enhancement over a heated cylinder oscillating with small amplitude in streamwise direction. ASME Journal of Heat Transfer 123, 1139–1148.

Griffin, O.M., 1995. A note on bluff body vortex formation. Journal of Fluid Mechanics 284, 217–224.

Griffin, O.M., Hall, H.S., 1991. Vortex shedding lock-on and flow control in bluff body wakes—review. ASME Journal of Fluids Engineering 113, 283–291.

Griffin, O.M., Ramberg, S.E., 1976. Vortex shedding from a cylinder vibrating in line with an incident uniform flow. Journal of Fluid Mechanics 75, 526–537.

Hardwick, J.D., Wootton, L.R., 1973. The use of model and full-scale investigations on marine structures. In: International Symposium for Vibration Problems in Industry, Keswick, UK, Paper 127.

Jauvtis, N., Williamson, C., 2004. The effect of two degrees of freedom on vortex-induced vibration at low mass and damping. Journal of Fluid Mechanics 509, 23–62.

King, R., 1977. A review of vortex shedding research and its application. Ocean Engineering 4, 141–171.

King, R., Prosser, M.J., Johns, D.J., 1973. On vortex excitation of model piles in water. Journal of Sound and Vibration 29, 169–188.

Konstantinidis, E., Balabani, S., 2006. The effect of forcing amplitude on vortex strength, drag and Reynolds stresses in the wake of a cylinder in oscillating flow. Presented at European Fluid Mechanics Conference EFMC6, Royal Institute of Technology, Stockholm, June 26–30.

Konstantinidis, E., Balabani, S., Yianneskis, M., 2003. The effect of flow perturbations on the near wake characteristics of a circular cylinder. Journal of Fluids and Structures 18, 367–386.

Konstantinidis, E., Balabani, S., Yianneskis, M., 2005a. Conditional averaging of PIV plane wake data using a cross-correlation approach. Experiments in Fluids 39, 38–47.

Konstantinidis, E., Balabani, S., Yianneskis, M., 2005b. The timing of vortex shedding in a cylinder wake imposed by periodic inflow perturbations. Journal of Fluid Mechanics 534, 45–55.

Lecointe, Y., Piquet, J., 1989. Flow structure in the wake of an oscillating circular cylinder. ASME Journal of Fluids Engineering 111, 139–148.

Liu, S., Fu, S., 2003. Regimes of vortex shedding from an in-line oscillating circular cylinder in uniform flow. ACTA Mechanica Sinica 19, 118–126.

Naudascher, E., 1987. Flow-induced streamwise vibrations of structures. Journal of Fluids and Structures 1, 265–298.

Nishihara, T., Kaneko, S., Watanabe, T., 2005. Characteristics of fluid dynamic forces acting on a circular cylinder oscillated in the streamwise direction and its wake patterns. Journal of Fluids and Structures 20, 505–518.

Norberg, C., 1998. LDV measurements in the near wake of a circular cylinder. In: Bearman, P.W., Williamson, C.H.K. (Eds.), Advances in the Understanding of Bluff Body Wakes and Vortex-Induced Vibration, Washington, DC.

Norberg, C., 2003. Fluctuating lift on a circular cylinder: review and new measurements. Journal of Fluids and Structures 17, 57–96.

Oengören, A., Ziada, S., 1998. An in-depth study of vortex shedding, acoustic resonance and turbulent forces in normal triangle tube arrays. Journal of Fluids and Structures 12, 717–758.

Okajima, A., Yasuda, T., Iwasaki, T., 2000, Flow visualization of in-line oscillation of a cylinder with circular or rectangular section. In: FLUCOME2000, F1048, Sherbrooke, QC, Canada, August 13–17.

Okajima, A., Kosugi, T., Nakamura, A., 2002. Flow-induced in-line oscillation of a circular cylinder in a water tunnel. ASME Journal of Pressure Vessel Technology 124, 89–96.

Ongoren, A., Rockwell, D., 1988. Flow structure from an oscillating cylinder. Part 2. Mode competition in the near wake. Journal of Fluid Mechanics 191, 225–245.

Prasad, A., Williamson, C.H.K., 1997. The instability of the shear layer separating from a bluff body. Journal of Fluid Mechanics 333, 375–402.

Raffel, M., Willert, C., Kompenhans, J., 1998. Particle Image Velocimetry: A Practical Guide. Springer, Berlin.

Rajagopalan, S., Antonia, R.A., 2005. Flow around a circular cylinder—structure of the near wake shear layer. Experiments in Fluids 38, 393–402.

Rao, P.M., Kuwahara, K., Tsuboi, K., 1992. Simulation of unsteady viscous flow around a longitudinally oscillating circular cylinder in a uniform flow. Applied Mathematical Modelling 16, 26–35.

Sarpkaya, T., 2004. A critical review of the intrinsic nature of vortex-induced vibrations. Journal of Fluids and Structures 19, 389–447.

Williams, T.C., Hargrave, G.K., Halliwell, N.A., 2003. The development of high-speed particle image velocimetry (20 kHz) for large eddy simulation code refinement in bluff body flows. Experiments in Fluids 35, 85–91.

Williamson, C.H.K., 1996. Vortex dynamics in the cylinder wake. Annual Review of Fluid Mechanics 28, 477–539.

Williamson, C.H.K., Roshko, A., 1988. Vortex formation in the wake of an oscillating cylinder. Journal of Fluids and Structures 2, 355–381.

Xu, S.J., Zhou, Y., Wang, M.H., 2006. A symmetric binary-vortex street behind a longitudinally oscillating cylinder. Journal of Fluid Mechanics 556, 27–43.

Yokoi, Y., Kamemoto, K., 1994. Vortex shedding from an oscillating circular cylinder in a uniform flow. Experimental Thermal Fluid Science 8, 121–127.

Zdravkovich, M.M., 1997. Flow Around Circular Cylinders, vol. 1. Oxford University Press, Oxford.

Zhou, C.Y., Graham, J.M.R., 2000. A numerical study of cylinders in waves and currents. Journal of Fluids and Structures 14, 403–428.